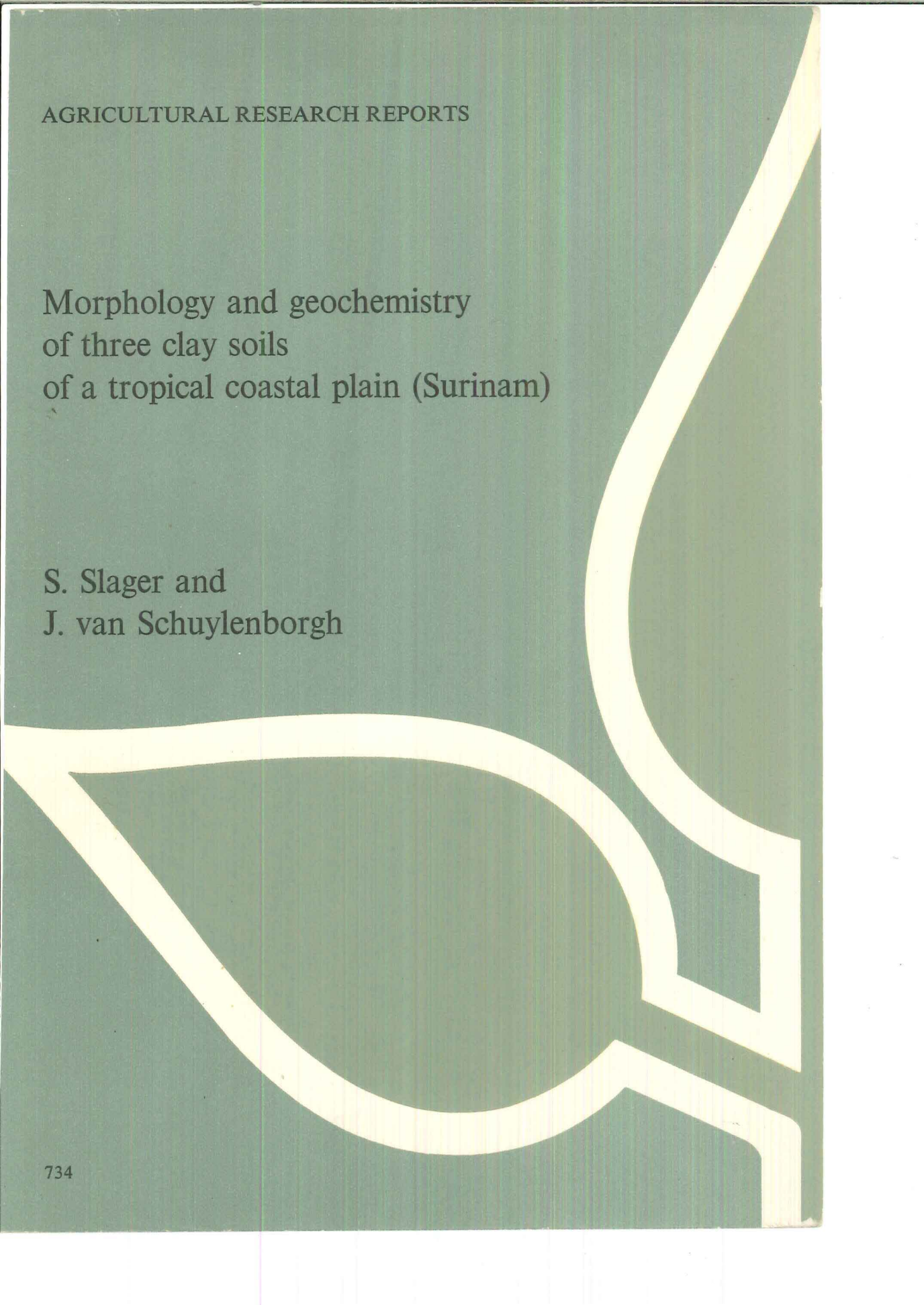
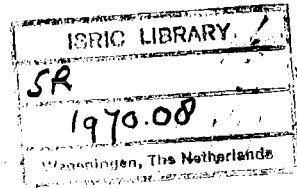


AGRICULTURAL RESEARCH REPORTS

Morphology and geochemistry  
of three clay soils  
of a tropical coastal plain (Surinam)

S. Slager and  
J. van Schuylenborgh





**Morphology and geochemistry of three clay soils of  
a tropical coastal plain (Surinam)**

Scanned from original by ISRIC – World Soil Information, as ICSU World Data Centre for Soils. The purpose is to make a safe depository for endangered documents and to make the accrued information available for consultation, following Fair Use Guidelines. Every effort is taken to respect Copyright of the materials within the archives where the identification of the Copyright holder is clear and, where feasible, to contact the originators. For questions please contact [soil.isric@wur.nl](mailto:soil.isric@wur.nl) indicating the item reference number concerned.

ISN 16466

*Verlagen van Landbouwkundige Onderzoeken 734*

S. Slager and J. van Schuylenborgh

*Department of Soil Science, Agricultural University,  
Wageningen, The Netherlands*

## Morphology and geochemistry of three clay soils of a tropical coastal plain (Surinam)



1970 *Centre for Agricultural Publishing and Documentation*

*Wageningen*

ISBN 90 220 0194 6

UDC 631.42 (883)

© Centrum voor Landbouwpublicaties en Landbouwdocumentatie, Wageningen, 1970.

Niets uit deze uitgave mag worden verveelvoudigd en/of openbaar gemaakt door middel van druk, fotocopie, microfilm of op welke andere wijze ook, zonder voorafgaande schriftelijke toestemming van de uitgever.

No part of this book may be reproduced and/or published in any form, photoprint, microfilm or by any other means without written permission from the publishers.

# Contents

<b>1</b>	<b>Introduction</b>	<b>1</b>
<b>2</b>	<b>Methods</b>	<b>1</b>
<b>3</b>	<b>Observations and analytical data</b>	<b>2</b>
3.1	Soil-forming factors	2
3.2	Macromorphology	3
3.3	Micromorphology	4
3.4	Geochemistry	5
<b>4</b>	<b>Discussion</b>	<b>12</b>
4.1	Interpretation of the observations	12
4.2	Interpretation of the chemical data	14
<b>5</b>	<b>Soil classification</b>	<b>18</b>
<b>6</b>	<b>Summary</b>	<b>19</b>
<b>7</b>	<b>Acknowledgments</b>	<b>19</b>
	<b>Appendix 1</b>	<b>21</b>
	<b>Appendix 2</b>	<b>29</b>
	<b>Appendix 3</b>	<b>31</b>
	<b>References</b>	<b>33</b>

## 1 Introduction

Surinam can be divided into three landscape belts: the Interior Uplands in the south, the Cover Landscape and the Coastal Plain (Van der Eyck, 1957). The Coastal Plain forms a belt about 10 km wide in the east and about 70 km wide in the west. It can be subdivided into the Pleistocene Old Coastal Plain in the south and the Holocene Young Coastal Plain in the north, both mainly consisting of marine sediments. Both are traversed by rivers bordered by fluvial and fluvio-marine deposits. The marine deposits of the Old Coastal Plain, labelled Coropina Series (Montagne, 1964; Brinkman & Pons, 1968), consist of dissected plains of silty clay soils with impeded drainage. At the northern edge they are bordered by strips of lighter textured soils with good to excessive drainage. The Young Coastal Plain consists of swamps with heavy clay soils alternating with ridges parallel to the sea and consisting of sand and shell soils.

A preliminary investigation of the soils of the Coastal Plain has not shown large variation in properties of the clay soils therein: when using a soil auger few differences were found except those in mottling colours and ripening. More detailed investigations, however, reveal considerable differences. The present paper describes such an investigation.

## 2 Methods

Three soils were studied: two clay soils of the Young Coastal Plain and one silty clay soil of the Old Coastal Plain. The profiles were described according to US Soil Survey Staff (1962). Where necessary, soil structure descriptions were extended, using the scheme of Jongerius (1957). Biopore nomenclature followed the scheme of Slager (1966). The soils were classified according to the scheme developed by the US Soil Survey Staff (1960, 1967). The quantitative microscopical pyrite determinations were performed according to a method which was based on that of Pons (1964). The thin sections were like those which Jongerius & Heintzberger (1964) called mammoth-size thin sections and they were prepared in a similar way. The descriptions of the thin sections is according to Brewer (1964). The chemical analyses were performed in the way described by Bouma *et al.* (1968), but with additional determination of FeO, P<sub>2</sub>O<sub>5</sub>, K<sub>2</sub>O and Na<sub>2</sub>O in the residue after hydrofluoric acid destruction of soil and clay separates. The clay fractions were X-rayed to estimate their qualitative composition. Furthermore the normative mineralogical compositions of clay separates and of the soils were

calculated according to rules developed by van der Plas & van Schuylenborgh (1970).

### 3 Observations and analytical data

For this study some tens of profiles were studied in the field. Three soils were selected for further investigation. Profile descriptions and descriptions of thin sections are given in Appendix I. The analytical data are given in Tables 1 to 18. In the following sections these data will be discussed.

#### 3.1 Soil-forming factors

The *climate* of the area has the following characteristics. Annual precipitation reaches 2200 mm, with less than 100 mm precipitation only in two or three months each year. The average temperature is 27°C with very small daily and monthly variation.

The three soils form a *chronosequence*. According to Brinkman & Pons (1968) the age increases in the following sequence: Ma Retraite, Santo, Kennedy Highway. The first and second soils are Holocene and belong to the Demerara Series and have developed in Coronie deposits, the first in the Comowine phase, the second in the Wanica phase. The Ma Retraite soil belongs to the oldest soils of the Comowine phase: this formation is supposed to have started some 1000 years ago. The Ma Retraite soil was almost constantly flooded with brackish or saline water till it was reclaimed some years ago, so that soil formation is still in its initial stage. The Santo soil originates probably from about the middle of the Wanica phase. This phase began about 6000 years ago. The Santo soil is consequently 4000 to 5000 years old. The Kennedy Highway soil is Pleistocene. Datings for this soil are still tentative.

The *parent materials* of the soils show much resemblance. According to Veen (1968, personal communication), both the clay mineral associations and the ratios between the clay minerals of the sediments of the Old and Young Coastal Plain were the same originally. Levelt & Quakernaat (1968) express the same opinion. The three soils have little or no sand (see Tables 1, 7, 13). The Ma Retraite soil and the Santo soil have a clay texture; the Kennedy Highway soil has a silty-clay texture in the subsoil.

The *topography* of the soils is very similar. Macrorelief is slightly ponded in the youngest soils and flat in the older one. Microrelief consists of a man-made system of shallow ditches every 6 or 8 metres, alternated with slightly convex beds. Physiography is different, but the differences are only reflected in the macrorelief. The altitudes are different too, but these differences are not believed to have had great effect on the soil-forming processes. The main factor influenced by the topography is the external hydrology of the soils. All three soils are (or were till some years ago) insufficiently drained and periodically flooded. The duration of

inundation, the water level above soil surface, and the salinity of the inundation water were different. Before reclamation, the Ma Retraite soil was flooded for most of the year with brackish to saline water, which reached a metre deep. The Santo soil, which was reclaimed some years earlier, was flooded for some 6 months per year with 20 to 30 cm fresh water. In the Kennedy Highway area, real swamp conditions have always been rare.

The influence of *vegetation* and *man* on the formation of the three soils under consideration do not differ much. The vegetation has changed from an original mangrove vegetation during sedimentation, into a low open swamp forest on the younger soils and a mesophytic to hydrophytic tropical rain-forest on the older soils. An intermediate stage of grass-swamp or low and open swamp forest may have occurred. Finally man has destroyed all natural vegetation when reclaiming these soils. The purpose of reclamation was to improve the hydrological conditions: only on the Ma Retraite soil has this succeeded.

Thus the main difference in soil-forming factors of the three soils is age, and to a lesser extent topography which has influenced drainage.

### 3.2 Macromorphology

Differences in soil texture are small (see also Tables 1, 7, 13), differences in soil structure, however, are considerable. This is particularly true for the size-class distributions and abundance of biopores. In these heavy-textured soils, fissures

Table 1. Some characteristics of the Ma Retraite soil.

Horizon	Texture			pH		C (%)	'Free Fe <sub>2</sub> O <sub>3</sub> ' (%)
	% >50 $\mu$	50-2 $\mu$	<2 $\mu$	H <sub>2</sub> O	0.01 M CaCl <sub>2</sub>		
A1g	0.1	33.1	66.8	4.4	3.6	7.8	3.2
B1g	0.1	32.2	67.7	4.1	3.3	4.1	3.6
B21g	0.4	36.9	62.7	3.9	3.1	2.1	5.5
B22g	0.3	37.2	62.5	3.4	3.2	1.5	5.5
B3g	0.1	36.9	63.0	6.7	6.1	1.6	4.9

develop during the dry period. They are absent during the wet season and do not seem to contribute to drainage. Single or compound packing voids are absent, except in the surface soils. So all percolation is through biopores. In the Ma Retraite soil many large and fine biopores are present, resulting in an extremely high permeability (over 10 m water per day). In the Santo soil only few large and fine biopores occur, so that permeability is low (less than 50 cm per day). The Kennedy Highway soil contains only very few fine biopores and permeability is low.

Below a shallow surface soil with biogenic structural elements (Slager, 1966),

all three soils show a sequence of physiogenic structures. The latter consist of angular-blocky elements as parts of compound prisms; sometimes single prisms are present. There is a general tendency towards larger elements and less fragmentation with increasing depth. In the Kennedy Highway profile, fragmentation has gone so far that compound elements are totally absent.

Differences in consistence are large, both within and between the profiles. Ripening increases from the Ma Retraite soil, through the Santo soil to the Kennedy Highway soil. The first two soils have  $n$  values higher than 0.5 between 20 and 50 cm (Kamerling, 1966; personal communication). The  $n$  values in the Kennedy Highway soil are much lower. Within the Ma Retraite and the Santo soil  $n$  values increase from the top to the bottom.

Soil matrix colours indicate periodic reductive conditions in all three soils. Chromas are only in some of the surface horizons higher than 2, as a rule combined with mottling; below the surface horizons they are always lower than or equal to 2. Chromas normally tend to decrease with depth. Hues tend to change from 10YR to 5Y or neutral with depth. Significant differences in matrix colours were not observed.

Peaty surface layers in the two younger soils also indicate wet conditions.

Mottling is rather different in the three soils and was used in Surinam to differentiate the soils in the field for soil survey purposes (van Amson, 1966). Rather characteristic mottles and very soft iron pipes with a colour of 10YR 4/4 occur in the B horizon of the Ma Retraite soil. The B horizon of the Santo soil has iron mottles of a colour 10YR 6/8. The  $B_{2tg}$  horizon of the Kennedy Highway soil contains soft and hard iron nodules with red (10R 4/8) and dark-red (7.5R 3/8) colours.

The pyrite contents differ widely. The surface layer of the Ma Retraite soil contains a lot of it (several percent by weight); deeper, however, the pyrite content is low and constant (0.2-0.3 % by weight) and does not increase when passing into the totally reduced subsoil. A similar trend was observed in the Santo soil but here the pyrite content of the surface layer does not exceed 1 % by weight. The Kennedy Highway soil contains no pyrites. We can conclude that the main differences in macromorphological properties are (from the younger to the older soils): decrease in bioporosity and permeability; increase in fragmentation of soil structure (change from single prisms to fine angular-blocky elements); transition from soft mottles to hard nodules; change in colour of these mottles from yellowish brown through yellow to dark-red; decrease in pyrite content.

### 3.3 Micromorphology

The plasmic fabrics of the soils are characterized by plasma separations. In most of the sections clinobimasepic and channelvosepic plasmic fabrics were noticed. The oldest soils also contain planarvosepic plasmic fabrics. In the youngest soils the channelvosepic plasmic fabric seems to replace the clinobimasepic plasmic

fabric with depth. The same transition was observed with age of the soils; in the oldest soils the clinobimasepic plasmic fabric was replaced by the planarvosepic plasmic fabric.

The basic structure is such that the skeleton grains are almost entirely restricted to the silt fraction. Their distribution is a random one. In most of the sections microchannels and macrochannels and microplanes and macroplanes (skew and craze planes) were observed. In the observed soils channels gradually replaced the planes with increasing depth. The reverse was observed with increasing age of the soils.

In the young soils, the elementary structure changed with depth from glaeular, fractured or crazed porphyroskelic to a subcutanic channelled porphyroskelic. The reverse could be observed with increasing age of the soils. Both the subcutanic features and the glaeules consisted of accumulations of iron compounds.

Several types of iron pedological features occur in these soils. Moreover, evidence of clay illuviation was found in some of the studied soils. X-ray analysis showed that the iron compounds change from amorphous ferric hydroxides to well crystallized goethite with increasing age of the soils. In the youngest soils both channel neocutans and nodules of iron were found. With increasing depth the channel neoferrans gradually replace the ferric nodules. Colours of both range from yellow to orange-brown. In the older soils channel neoferrans, nodules and ferric crystal sheets were observed, the latter two groups exceeding the former group in abundance. The iron compounds change from yellow and orange-brown to very deep-red.

Evidences of recent or fossil clay illuviation tend to increase from the youngest to the oldest soil. No argillans or papules were found in the Ma Retraite soil. In the Santo soil ( $B_{1g}$  horizon) one or two ferri-argillans were noticed, together with the same number of papules. Many papules occurred in the  $B_{2lg}$  horizon of the Kennedy Highway soil (some 4 % of the surface area of the thin section).

We conclude that from young to old the following changes occur: from channelvosepic to clinobimasepic and planarvosepic plasmic fabrics; from channels to skew planes; from yellow orange channel neoferrans to deep red ferric glaeules and ferric crystal sheets; increasing evidence of (recent or fossil) clay illuviation.

### 3.4 Geochemistry

The geochemistry of the soils will be discussed in detail for each profile separately, starting with the Ma Retraite soil, the youngest one. Table 1 shows that this young soil has a very low pH, concordant with the data on pyrite content (Section 3.2). The lowest horizon has a slightly acid reaction, which shows that either its pyrite content was extremely low or that it has not yet been sufficiently oxidized (see profile description). Furthermore both Table 1 and the micro-morphology show that clay has not yet migrated. This might have two reasons: (a) the youth of the profile; (b) the rapid decrease of the pH in this soil through

Table 2. Cation-exchange characteristics of the Ma Retraite soil (meq/100 g soil).

Horizon	Exchangeable cations					CEC	Base saturation %
	Ca <sup>2+</sup>	Mg <sup>2+</sup>	K <sup>+</sup>	Na <sup>+</sup>	Al <sup>3+</sup> +H <sup>+</sup>		
A1g	6.0	12.4	1.3	0.5	6.0	25.0	75
B1g	4.5	10.8	0.5	0.5	11.6	28.1	58
B21g	3.0	8.5	0.5	0.9	14.9	25.7	42
B22g	2.8	7.7	0.5	0.3	14.8	25.6	42
B3g	10.1	15.3	1.2	1.7	0.0	25.6	100

oxidation of pyrite. If the latter the clay was transformed into a strongly coagulated and immobile Al-Mg-Ca-clay (Table 2). The high content of exchangeable Mg (Table 2) indicates that montmorillonite is an important clay mineral in this soil, and became unstable upon acidification and consequently released Mg from its lattice (van Es & van Schuylenborgh, 1967; Barshad, 1960). The high cation-exchange capacity of the soil is further indication of a considerable content of montmorillonite.

Table 1 shows further that iron is mobile in this soil, as 'free Fe<sub>2</sub>O<sub>3</sub>' content increases with depth to a maximum in B<sub>21g</sub> and B<sub>22g</sub>. The mobility of iron is easily understandable, as the profile is alternately in oxidized and reduced state. For a discussion, the reader is referred to Bouma *et al.* (1968) and to Section 4.2.

The chemical composition of the clay fractions of the profile and the molar silica sesquioxide ratios in Table 3 show that the clay composition is fairly constant throughout the profile, except for Fe<sub>2</sub>O<sub>3</sub>. The latter result is consistent with the data on 'free Fe<sub>2</sub>O<sub>3</sub>' in Table 1. The clays of the surface layers are slightly richer in Al<sub>2</sub>O<sub>3</sub> and SiO<sub>2</sub> than below. The molar silica/Al<sub>2</sub>O<sub>3</sub> ratio is constant whereas the molar Al<sub>2</sub>O<sub>3</sub>/Fe<sub>2</sub>O<sub>3</sub> and SiO<sub>2</sub>/Fe<sub>2</sub>O<sub>3</sub> ratios indicate a higher mobility of iron than of Al-bearing and Si-bearing constituents of the clay.

X-ray analysis of the clay revealed the presence of kaolinite, smectite, illite, iron hydroxides and quartz as did the goethite norm composition calculated from the data of Table 3 (see also Table 4). Table 4 shows that composition is fairly constant, except again for the goethite content. Close examination of the table reveals, however, that certain transformations were initiated. The smectite content decreases and the kaolinite and silica contents increase from the bottom of the profile to the top. This means that some smectite was transformed into kaolinite, whilst silica enriched residually. This phenomenon will be discussed with the older profiles.

The chemical composition of the soil is also fairly constant, except again for Fe<sub>2</sub>O<sub>3</sub> (Table 5). In addition, MgO seems to have been leached, indicating that some Mg mineral (chlorite as shown by X-rays) was unstable during soil formation. The normative mineralogical composition, represented in Table 6, shows that the sodium feldspars, muscovite and chlorite were unstable and slightly decomposed during soil formation.

Table 3. Chemical composition of the clay fractions of the Ma Retraite soil (weight percentage) and the molar silica/sesquioxide ratios.

	A1g	B1g	B21g	B22g	B3g		A1g	B1g	B21g	B22g	B3g
SiO <sub>2</sub>	49.5	48.2	47.4	47.6	47.8	MnO	tr.	tr.	tr.	tr.	tr.
Al <sub>2</sub> O <sub>3</sub>	25.8	25.6	24.7	24.9	25.0	P <sub>2</sub> O <sub>5</sub>	0.2	0.2	0.3	0.3	0.3
Fe <sub>2</sub> O <sub>3</sub>	5.8	6.6	8.5	8.5	8.9	H <sub>2</sub> O+	11.6	11.1	11.0	11.0	10.7
FeO	0.5	0.5	0.5	0.6	0.5						
CaO	0.2	0.2	0.2	0.1	0.2	SiO <sub>2</sub> /R <sub>2</sub> O <sub>3</sub>	2.8	2.7	2.6	2.6	2.6
MgO	1.3	1.3	1.4	1.4	1.4	SiO <sub>2</sub> /Al <sub>2</sub> O <sub>3</sub>	3.3	3.2	3.3	3.3	3.3
Na <sub>2</sub> O	0.3	0.3	0.3	0.3	0.3	SiO <sub>2</sub> /Fe <sub>2</sub> O <sub>3</sub>	21	17	14	13	13
K <sub>2</sub> O	2.6	2.6	2.6	2.6	2.6	Al <sub>2</sub> O <sub>3</sub> /Fe <sub>2</sub> O <sub>3</sub>	6.3	5.5	4.2	4.1	4.1
TiO <sub>2</sub>	0.9	0.8	0.8	0.8	0.9						

Table 4. Goethite normative composition of the clay fractions of the Ma Retraite soil (weight percentage).

Horizon	Silica	Kaolinite	Illite	Smectite	Goethite	Strengite	Rutile (anatase)
A1g	7.4	33.4	22.4	29.2	6.2	0.6	0.9
B1g	6.5	32.7	22.6	29.5	7.3	0.6	0.9
B21g	5.7	29.2	22.6	31.4	9.4	0.8	0.9
B22g	5.5	29.1	22.4	32.0	9.3	0.8	0.9
B3g	5.7	28.5	22.4	31.9	9.7	0.8	1.0

Table 5. Chemical composition of the Ma Retraite soil (weight percentage) and the molar relation silica/sesquioxide.

	A1g	B1g	B21g	B22g	B3g		A1g	B1g	B21g	B22g	B3g
SiO <sub>2</sub>	50.2	52.3	52.0	53.9	53.7	MnO	0.1	tr.	0.1	0.1	0.2
Al <sub>2</sub> O <sub>3</sub>	20.5	22.4	22.1	22.1	21.3	P <sub>2</sub> O <sub>5</sub>	0.3	0.2	0.2	0.2	0.2
Fe <sub>2</sub> O <sub>3</sub>	4.8	5.9	7.7	7.6	6.9	loss on					
FeO	0.9	0.7	0.6	0.7	1.0	ignition	17.9	12.9	9.7	9.9	9.6
CaO	0.7	0.4	0.5	0.6	0.8						
MgO	1.3	1.4	1.6	1.6	2.1	SiO <sub>2</sub> /R <sub>2</sub> O <sub>3</sub>	3.5	3.4	3.2	3.4	3.4
Na <sub>2</sub> O	0.7	0.8	0.8	1.0	1.0	SiO <sub>2</sub> /Al <sub>2</sub> O <sub>3</sub>	4.2	4.0	4.0	4.1	4.3
K <sub>2</sub> O	2.6	2.8	2.8	2.8	2.8	SiO <sub>2</sub> /Fe <sub>2</sub> O <sub>3</sub>	23	22	17	17	17
TiO <sub>2</sub>	0.9	0.9	0.9	0.9	0.9	Al <sub>2</sub> O <sub>3</sub> /Fe <sub>2</sub> O <sub>3</sub>	5.5	5.6	4.3	4.2	4.0

Table 6. Normative mineralogical composition of the Ma Retraite soil (weight percentage).

Horizon	Silica	Albite	Chlorite	Kaolinite	Illite	Smectite	Goethite	Strengite	Rutile	Misc.
A1g	15.6	5.4	0.0	22.3	21.8	19.5	5.2	1.1	1.1	8.0
B1g	16.9	5.1	1.4	22.1	23.2	20.0	6.5	0.6	1.1	2.2
B21g	17.1	5.2	2.1	18.3	24.1	19.7	8.6	0.5	1.0	3.4
B22g	17.2	6.3	2.0	18.2	24.0	20.0	8.0	0.5	1.0	2.8
B3g	14.4	7.0	2.2	18.0	24.4	21.1	7.6	0.5	1.0	0.7

Table 7. Some characteristics of the Santo soil.

Horizon	Texture			pH		C (%)	'Free Fe <sub>2</sub> O <sub>3</sub> ' (%)
	% >50 $\mu$	50-2 $\mu$	<2 $\mu$	H <sub>2</sub> O	0.01 M CaCl <sub>2</sub>		
A1g	0.2	29.5	70.3	3.7	3.2	5.4	0.7
B1g	0.2	30.9	68.9	4.6	4.0	2.8	1.4
B2g	0.6	38.2	61.2	4.6	4.0	0.9	5.7
B3g	0.3	37.6	62.1	6.2	5.9	0.4	4.9

Thus soil-forming processes in this soil are still in the initial stage, although certain tendencies should be noted: transformation of albite, chlorite and muscovite; transformation of smectite into kaolinite; translocation of iron and residual enrichment of free silica.

The Santo soil, which is older than the Ma Retraite soil, but developed in similar parent material (see Section 3.1), shows the same tendencies, though more pronounced. There are some differences because of the original lower pyrite content. Hence this soil is not as acid as the youngest soil and does not contain so much exchangeable Al (see Table 8). The cation-exchange capacity is lower than in the Ma Retraite soil which indicates that the clay composition differs

Table 8. Cation-exchange characteristics of the Santo soil (meq/100 g soil).

Horizon	Exchangeable cations					CEC	Base saturation %
	Ca <sup>2+</sup>	Mg <sup>2+</sup>	K <sup>+</sup>	Na <sup>+</sup>	Al <sup>3+</sup> +H <sup>+</sup>		
A1g	3.4	1.4	0.4	0.2	18.7	20.2	7
B1g	10.5	5.2	0.5	0.3	2.9	17.5	83
B2g	9.6	5.2	0.5	0.6	2.3	16.4	86
B3g	8.2	6.1	0.4	0.6	0.5	18.6	98

Table 9. Chemical composition of the clay separates of the Santo soil (weight percentage) and the molar relation silica/sesquioxide.

	A1g	B1g	B2g	B3g		A1g	B1g	B2g	B3g
SiO <sub>2</sub>	53.3	51.0	49.2	49.9	MnO	tr.	tr.	tr.	tr.
Al <sub>2</sub> O <sub>3</sub>	27.2	26.6	24.3	24.3	P <sub>2</sub> O <sub>5</sub>	0.1	0.1	0.1	0.1
Fe <sub>2</sub> O <sub>3</sub>	4.8	5.5	11.3	10.3	H <sub>2</sub> O+	11.4	10.8	10.4	10.4
FeO	0.2	0.2	0.4	0.3					
CaO	0.0	0.0	0.0	0.0	SiO <sub>2</sub> /R <sub>2</sub> O <sub>3</sub>	3.0	2.9	2.6	2.7
MgO	1.0	1.0	1.0	1.2	SiO <sub>2</sub> /Al <sub>2</sub> O <sub>3</sub>	3.3	3.3	3.4	3.5
Na <sub>2</sub> O	0.3	0.3	0.3	0.4	SiO <sub>2</sub> /Fe <sub>2</sub> O <sub>3</sub>	29	24	11	13
K <sub>2</sub> O	1.8	2.1	2.1	2.4	Al <sub>2</sub> O <sub>3</sub> /Fe <sub>2</sub> O <sub>3</sub>	8.6	7.3	3.2	3.6
TiO <sub>2</sub>	1.1	0.9	0.9	0.9					

Table 10. Goethite normative composition of the clay fractions of the Santo soil (weight percentage).

Horizon	Silica	Kaolinite	Illite	Smectite	Goethite	Strengite	Rutile (anatase)
A1g	16.5	45.4	15.2	20.5	5.3	0.1	1.1
B1g	11.2	42.6	17.8	21.2	6.1	0.1	0.9
B2g	11.2	34.3	17.7	23.3	12.6	0.1	0.9
B3g	10.8	31.2	20.5	24.9	11.5	0.1	0.9

quantitatively from that of the Ma Retraite soil. This becomes very clear when calculating the goethite-normative composition of the clay from its chemical composition (Tables 9, 10). Obviously smectite and illite have been partially transformed into kaolinite, while free silica was enriched residually. This tendency could already be seen in the Ma Retraite soil, but here the transformation is more pronounced. The lower cation-exchange capacity was explained by the much higher kaolinite content than in the first profile. Because of the difference in age, iron has

Table 11. Chemical composition of the Santo soil (weight percentage) and the molar relation silica/sesquioxide.

	A1g	B1g	B2g	B3g		A1g	B1g	B2g	B3g
SiO <sub>2</sub>	52.5	57.2	58.0	59.5	MnO	0.1	0.1	0.1	0.2
Al <sub>2</sub> O <sub>3</sub>	21.6	24.0	20.8	20.2	P <sub>2</sub> O <sub>5</sub>	0.2	0.1	0.1	0.1
Fe <sub>2</sub> O <sub>3</sub>	2.8	4.2	7.5	6.9	loss on				
FeO	0.5	0.4	0.8	0.8	ignition	16.7	8.7	7.4	7.3
CaO	0.2	0.3	0.2	0.2					
MgO	0.5	0.6	0.7	0.9	SiO <sub>2</sub> /R <sub>2</sub> O <sub>3</sub>	3.8	3.6	3.8	4.0
Na <sub>2</sub> O	0.4	0.5	0.7	0.7	SiO <sub>2</sub> /R <sub>2</sub> O <sub>3</sub>	4.1	4.1	4.7	5.0
K <sub>2</sub> O	1.6	2.0	2.0	2.1	SiO <sub>2</sub> /Fe <sub>2</sub> O <sub>3</sub>	45	35	18	19
TiO <sub>2</sub>	0.9	1.0	0.9	0.9	Al <sub>2</sub> O <sub>3</sub> /Fe <sub>2</sub> O <sub>3</sub>	11	8.6	3.8	3.9

Table 12. Normative mineralogical composition of the Santo soil (weight percentage).

Horizon	Silica	Albite	Chlorite	Kaolinite	Illite	Smectite	Goethite	Strengite	Rutile	Misc.
A1g	26.6	2.4	0.9	35.2	14.4	14.4	3.7	tr.	1.0	1.4
B1g	21.9	2.6	0.6	37.1	16.2	14.6	4.7	tr.	1.0	1.3
B2g	26.5	4.3	1.0	26.7	17.0	14.3	8.3	tr.	1.0	0.9
B3g	27.7	4.2	2.0	23.6	17.5	15.5	7.8	tr.	1.0	1.0

been translocated in considerably greater quantities.

Finally the chemical composition of the profile (Table 11) and, more specifically, the normative mineralogical composition (Table 12) show that albite has continued to be transformed; so has muscovite and chlorite. Consequently, the

silica content of the Santo soil is higher than that of the Ma Retraite soil.

Thus the same conclusions can be drawn about soil-forming processes as in the Ma Retraite soil; the transformations and translocations have proceeded considerably further because of age.

The oldest soil (Kennedy Highway) shows still stronger transformations and translocations and the soil-forming processes in this profile are more intricate than in the foregoing profiles. Table 13 shows that clay migration or clay destruction has occurred during soil formation. Thin-section analysis (see Section 3.3) showed that the clay occurs partly as papules, whereas clay coatings do not occur. So in earlier times in the genesis of this profile clay migration has taken place. In turn this means that the soil has not been acidified as rapidly as the preceding profiles; otherwise migration of clay would have been prevented by formation of Al clays. Consequently the pyrite content of the original material must have been very low. Upon continued soil formation, after the formation of the argillic B-horizon, the soil has become gradually more acid, the clay converted into Al clay and migration ceased (Table 14). Swelling and shrinkage (see profile description in Appendix 1: stress cutans) has destroyed the clay coatings so that they now occur as papules.

Table 14 shows further that the cation-exchange capacity of the soil is still lower than that in the preceding profiles, which means that the smectite content will be lower, which is to be expected.

Table 15 shows that iron moved markedly; it is much more mobile than the Al and Si bearing components of the clay. Moreover, the trend in the relation  $\text{SiO}_2/\text{Al}_2\text{O}_3$  shows that either some clay component has been destroyed with the subsequent leaching of one of the decomposition products ( $\text{Al}_2\text{O}_3$ ), or that a differential clay movement has taken place, in which kaolinite was more mobile than the clay minerals with more  $\text{SiO}_2$  relative to  $\text{Al}_2\text{O}_3$  ratios. This problem can only be solved with a quantitative mineralogical study of the clay separate. For this purpose the goethite normative composition of the clay fraction was calculated. Table 16 shows that the smectites were increasingly transformed into kaolinite and dissolved silica, which was leached. Free alumina is absent, so that a differential clay movement has taken place, in accordance with results of Hallsworth (1963).

Table 13. Some characteristics of the Kennedy Highway soil.

Horizon	Texture			pH		C (%)	'Free $\text{Fe}_2\text{O}_3$ ' (%)
	% >50 $\mu$	50-2 $\mu$	<2 $\mu$	H <sub>2</sub> O	0.01 M CaCl <sub>2</sub>		
A11	0.8	72.4	26.8	4.1	3.6	1.9	0.2
A12g	0.6	60.5	38.9	4.3	3.6	1.1	0.3
B1tg	0.9	50.8	48.3	4.5	3.6	0.6	3.2
B21tg	1.1	39.9	59.0	4.4	3.6	0.5	5.5
B22tg	7.0	49.4	43.6	4.4	3.6	0.4	9.7

Table 14. Cation-exchange characteristics of the Kennedy Highway soil (meq/100 g soil).

Horizon	Exchangeable cations					CEC	Base saturation %
	Ca <sup>2+</sup>	Mg <sup>2+</sup>	K <sup>+</sup>	Na <sup>+</sup>	Al <sup>3+</sup> +H <sup>+</sup>		
A11	1.1	0.3	0.1	0.2	5.2	6.9	24
A12g	1.1	0.4	0.1	0.2	6.2	7.9	21
B1tg	1.1	0.4	0.1	0.2	7.6	9.4	20
B21tg	1.1	0.3	0.1	0.2	9.0	10.7	16
B22tg	1.1	0.4	0.1	0.2	8.1	9.8	17

Table 15. Chemical composition of the clay separates of the Kennedy Highway soil (weight percentage) and the relation silica/sesquioxide.

	A11	A12g	B1tg	B21tg	B22tg		A11	A12g	B1tg	B21tg	B22tg
SiO <sub>2</sub>	51.9	50.4	47.0	44.2	45.6	MnO	tr.	tr.	tr.	tr.	tr.
Al <sub>2</sub> O <sub>3</sub>	30.3	31.3	30.8	30.1	28.9	P <sub>2</sub> O <sub>5</sub>	0.1	0.1	0.1	0.1	0.1
Fe <sub>2</sub> O <sub>3</sub>	2.7	3.0	6.3	8.9	9.0	H <sub>2</sub> O+	11.2	11.6	11.7	12.1	11.6
FeO	0.2	0.3	0.7	1.3	1.3						
CaO	0.0	0.0	0.0	0.0	0.0	SiO <sub>2</sub> /R <sub>2</sub> O <sub>3</sub>	2.8	2.6	2.3	2.1	2.2
MgO	0.6	0.6	0.6	0.5	0.6	SiO <sub>2</sub> /Al <sub>2</sub> O <sub>3</sub>	2.9	2.7	2.6	2.5	2.7
Na <sub>2</sub> O	0.2	0.2	0.2	0.2	0.2	SiO <sub>2</sub> /Fe <sub>2</sub> O <sub>3</sub>	50	43	18	12	12
K <sub>2</sub> O	2.0	1.9	1.9	1.9	2.0	Al <sub>2</sub> O <sub>3</sub> /Fe <sub>2</sub> O <sub>3</sub>	17	16	6.8	4.7	4.5
TiO <sub>2</sub>	1.6	1.4	1.2	0.9	0.9						

Table 16. Goethite normative clay composition of the Kennedy Highway soil (weight percentage).

Horizon	Silica	Kaolinite	Illite	Smectite	Goethite	Strengite	Rutile (anatase)
A11	10.7	54.7	16.3	13.7	2.9	0.2	1.6
A12g	7.5	57.8	15.9	14.0	3.2	0.2	1.4
B1tg	3.3	54.1	15.9	18.5	6.9	0.2	1.2
B21tg	0.0	51.1	16.4	21.6	9.9	0.2	0.9
B22tg	2.2	46.6	17.0	23.1	10.1	0.2	0.9

Table 17 shows that the alkalis and earth alkalis have been leached to a considerable extent. Minerals such as chlorite and albite, which were originally present, have therefore completely or nearly completely weathered. Because of the considerably advanced decomposition of the primary minerals and the migration and transformation of the clay minerals, the soil was residually enriched in silica, as evident from Table 18. In this table it seems as if the 2:1 lattice minerals were more mobile than kaolinite; this is, however, only apparently so, since the kaolinite

Table 17. Chemical composition of the Kennedy Highway soil (weight percentage) and the molar relation silica/sesquioxide.

	A11	A12g	B1tg	B21tg	B22tg		A11	A12g	B1tg	B21tg	B22tg
SiO <sub>2</sub>	82.2	77.9	70.2	62.1	64.9	MnO	tr.	tr.	tr.	tr.	tr.
Al <sub>2</sub> O <sub>3</sub>	8.6	12.6	15.5	17.1	15.3	P <sub>2</sub> O <sub>5</sub>	0.1	0.1	0.1	0.1	0.1
Fe <sub>2</sub> O <sub>3</sub>	1.1	1.6	4.5	7.1	10.4	loss on					
FeO	0.1	0.1	0.2	0.5	0.5	ignition	6.1	6.1	6.9	7.9	6.4
CaO	0.1	0.1	0.1	0.1	0.1						
MgO	tr.	0.1	0.1	0.2	0.2	SiO <sub>2</sub> /R <sub>2</sub> O <sub>3</sub>	15	9.8	6.5	4.9	5.0
Na <sub>2</sub> O	0.1	0.2	0.2	0.2	0.2	SiO <sub>2</sub> /Al <sub>2</sub> O <sub>3</sub>	16	11	7.7	6.2	7.2
K <sub>2</sub> O	0.6	0.9	1.1	1.1	1.3	SiO <sub>2</sub> /Fe <sub>2</sub> O <sub>3</sub>	208	154	42	23	16
TiO <sub>2</sub>	1.4	1.5	1.4	1.1	1.0	Al <sub>2</sub> O <sub>3</sub> /Fe <sub>2</sub> O <sub>3</sub>	13	15	5.4	3.7	2.3

Table 18. Normative mineralogical composition of the Kennedy Highway soil (weight percentage).

Horizon	Silica	Albite	Chlorite	Kaolinite	Illite	Smectite	Goethite	Strengite	Rutile	Misc.
A11	73.7	0.0	0.0	15.5	4.4	3.7	1.1	0.1	1.2	3.7
A12g	60.8	0.8	0.0	22.5	7.0	5.4	1.7	0.1	1.5	5.0
B1tg	48.3	0.8	0.0	26.1	9.3	8.9	4.9	0.1	1.4	5.1
B21tg	34.3	0.6	0.0	30.1	11.6	12.7	8.4	0.1	1.0	6.8
B22tg	42.2	0.8	0.0	23.3	10.6	10.1	11.5	0.1	0.9	5.0

is newly formed from smectite.

Thus the same processes acted in the genesis of this profile as in the two younger profiles. Besides, differential clay movement occurred, as kaolinite was more mobile than smectite or illite.

The three profiles form an ideal chronosequence, showing the disappearance of albite and chlorite with age, the decrease of smectite as it was transformed into kaolinite and the increasing translocation of iron. Further details on this point will be given in Section 4.2.

## 4 Discussion

### 4.1 Interpretation of the observations

Few of the properties of the soils of the Coastal Plain can be understood without knowing the conditions prevailing during sedimentation of the parent materials. Detailed data on this point have been given by Pons & Zonneveld (1955), Pons (1966), van Amson (1966) and Brinkman & Pons (1968). For the three soils these conditions can be described as follows.

The Ma Retraite and the Santo soil are marine soils, sedimented under constant

sea-level (Pons, 1966; Brinkman & Pons, 1968). The sediments were transported by the Guiana Current (Diephuis, 1966) and lacked lime. They were deposited in an *Avicennia nitida* vegetation, a mangrove vegetation with an extensive system of pneumatophores. These pneumatophores grow upwards with the rising mudflat, thus providing the *Avicennia* trees with oxygen under extremely wet conditions. It is probable that the channel neostrians result from the growth of these pneumatophores. The mud is constantly homogenized (Slager, 1966) by crabs, preventing stratification. When sedimentation continues uninterrupted, the *Avicennia* zone becomes wider and the trees gradually die on the landward side. The soil then is an almost completely reduced mud with high n values, poor in lime and pyrites, with a varying number of channels.

When the *Avicennia* vegetation disappears, a brackish herbaceous and shrubby swamp vegetation takes its place. Pyrite accumulates in a peaty surface layer. Such swamps may periodically dry out to some depth or remain wet throughout the year. In the first case part of the pyrite may oxidize in the dry season, but without strong acidification of the soil. In the same period the soil loses water irreversibly, ripens to some extent and the n value decreases.

Moreover, peptization of the clay and illuviation of s-matrix leads to compaction of the subsurface horizons as the biopores and fissures fill with s-matrix. New finer biopores, however, are formed by the swamp vegetation. Iron compounds are oxidized and iron hydroxides precipitate around biopores, forming channel neoferrans.

If the swamp remains wet throughout the year, pyrite continues to accumulate in the peaty surface soil. Also new fine root channels form. Ripening, illuviation of s-matrix and compaction, however, do not occur. Neither are iron compounds oxidized or iron hydroxides precipitated.

The transition from brackish swamp to freshwater swamp normally proceeds gradually. At Ma Retraite man has brought a sudden change. The swamp was a brackish one, wet almost throughout the year. The soil was before reclamation a homogeneous mud with high n values and many biopores surrounded by channel neostrians; there was little structural development and little oxidation of iron. Reclamation caused (a) irreversible loss of water, (b) formation of fissures and prisms and subsequent fragmentation of the prisms into angular-blocky structures, (c) rapid desalinization of the very porous soil, (d) oxidation of pyrites and acidification of the soil, (e) precipitation of the iron hydroxides along biopores (channel neoferrans, which were later on destroyed by swelling and shrinkage in this heavy clay soil to form ferric glaebules).

The Santo soil may have formed in the same way as the Ma Retraite soil. In fact a peaty surface layer low in pyrite was found, but s matrix was not illuviated. Thus the brackish swamp phase could not have lasted very long. The change from a brackish to a freshwater swamp has been more gradual than in the Ma Retraite soil. The Santo soil was reclaimed from a freshwater swamp. Some soil formation probably occurred during the freshwater swamp phase; most soil formation, how-

ever, has taken place since reclamation. Several processes are more advanced than in the Ma Retraite soil: ripening, fragmentation of prisms, formation of slickensides, destruction of biopores and neoferrans (due to swelling and shrinkage), and crystallization of the iron compounds.

Furthermore clay illuviation has started. However the soil is not so acid as at Ma Retraite soil, perhaps because of an originally lower pyrite content and a lower permeability.

The Kennedy Highway soil was assumed to have formed as an extremely acid cat clay (Brinkman & Pons, 1968). Although this may be true for the lower part of the deposits in which this soil was formed, it seems not to apply to the upper part. Probably this soil was formed from a sediment, deposited under an *Avicennia* vegetation as were the other two soils. The pyrite content must have been originally low, judging from the weak acidity. Its present properties show that the soil is much older than the other two soils. In particular clay illuviation is distinct, although, judged from the large number of papules and the absence of argillans, it is already fossil.

#### 4.2 Interpretation of the chemical data

To study the mineral transformations, reported in Section 3.4 and Tables 6, 12 and 18, the possible phases in the system  $\text{Na}_2\text{O} - \text{K}_2\text{O} - \text{MgO} - \text{FeO} - \text{Al}_2\text{O}_3 - \text{SiO}_2 - \text{H}_2\text{O}$  must be established and their stability relations studied. But this is not yet possible, as thermodynamic data are still unknown for several of the minerals.

We shall therefore simplify the system and study the stable phases in the  $\text{K}_2\text{O} - \text{Al}_2\text{O}_3 - \text{SiO}_2 - \text{H}_2\text{O}$  system. The following phases may occur in this system at  $25^\circ\text{C}$  and one atmosphere total pressure: potassium feldspar, muscovite (illite), pyrophyllite, kaolinite and gibbsite, while in solution  $\text{K}^+$ ,  $\text{H}^+$ , and  $\text{H}_4\text{SiO}_4$  occur. Pyrophyllite can be considered a substitute for montmorillonite as it forms one of the end members of the talc-montmorillonite-pyrophyllite series.

To delineate the stability of the various phases, we have to establish the equilibria between postassium feldspar and muscovite, potassium feldspar and pyrophyllite, muscovite and gibbsite, muscovite and kaolinite, pyrophyllite and kaolinite, muscovite and pyrophyllite, kaolinite and gibbsite, potassium feldspar and  $\text{H}_4\text{SiO}_4$ , and pyrophyllite and  $\text{H}_4\text{SiO}_4$ . As part of the silica in the profile is metastable as amorphous silica, the upper limit of dissolved silica is controlled by the solubility of the amorphous silica.

The reactions needed and their equilibria are given in Appendix 2, and the results are reported in Fig. 1, which shows that the transition of feldspars into muscovite and pyrophyllite can be explained in terms of a decreasing  $[\text{K}^+]/[\text{H}^+]$  ratio and decreasing silicic acid activity in the soil solution. As silicic acid is released, the increase in free silica can only be understood as residual. As the climate shows two dry periods (one pronounced), some of the  $\text{H}_4\text{SiO}_4$  may dry out irreversibly by evaporation. If so, part of the silica is metastable.

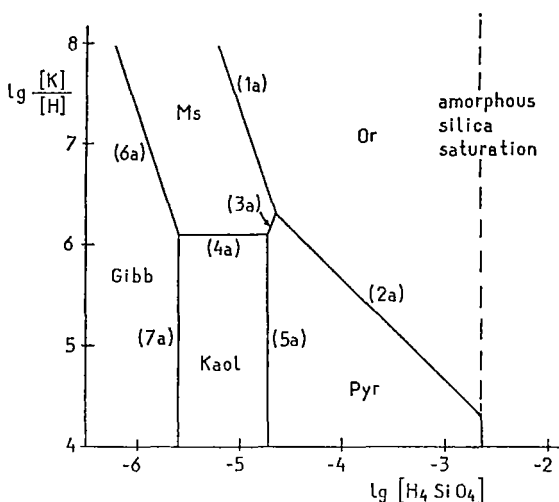


Fig. 1. Stable phases in the system  $K_2O-Al_2O_3-SiO_2-H_2O$  at  $25^\circ C$  and at 1 atm pressure.

The weathering process has not yet reached the stage at which kaolinite and muscovite become unstable and form gibbsite. For this the soil has to be much older.

Another process which is still occurring in some of the soils is oxidation of pyrite; considerable amounts of iron are also being translocated. As the pyrite content has originally been rather low (see Section 3.2), the soils have not turned into real cat clays, the more so as  $H^+$ , formed by the oxidation of the pyrite, is buffered by montmorillonite, as will be explained later.

The oxidation of pyrite has led to yellow, yellowish-brown, red and dark-red mottles, the red especially in the older soils. As the yellow colours are ascribed to the formation of jarosite (Schwertmann, 1961) (a substance found by X-ray analysis), it was of interest to study the stability relations of the various iron compounds in the soil and in the soil solution as a function of redox potential (Eh) and pH.

For this purpose the concentration of the dissolved sulphur compounds in the soil solution must be established, at least approximately. As in real cat clays this concentration varies between  $10^{-2}$  and  $3 \times 10^{-2}$  mol per litre and in rather strongly leached cat clays (pH between 4 and 6) between  $2$  and  $3 \times 10^{-3}$  mol per litre (Nhung & Ponnampereuma, 1966; van der Spek, 1950; Yoneda & Kawada, 1954), the value of  $10^{-3}$  mol per litre can be adopted in our considerations as the pyrite content was rather low originally. Under these conditions, the most important dissolved species are:  $Fe^{2+}$ ,  $FeSO_4^+$ ,  $FeSO_4^0$ ,  $H_2S$ ,  $HS^-$ ,  $HSO_4^-$  and  $SO_4^{2-}$  (van Breemen, 1968)\*. The solid iron species are:  $FeS_2$  (pyrite),  $FeS$  (hydrotroilite), rhombic S (Evans *et al.*, 1964; Berner, 1964),  $Fe_3(OH)_5(SO_4)_2 \cdot 2H_2O$  (jarosite;

\* Breemen, N. van (1968). Vorming en omzetting van sulfiden en sulfaten in zee-bodem sedimenten en kateklei gronden. M.Sc.Thesis, Wageningen.

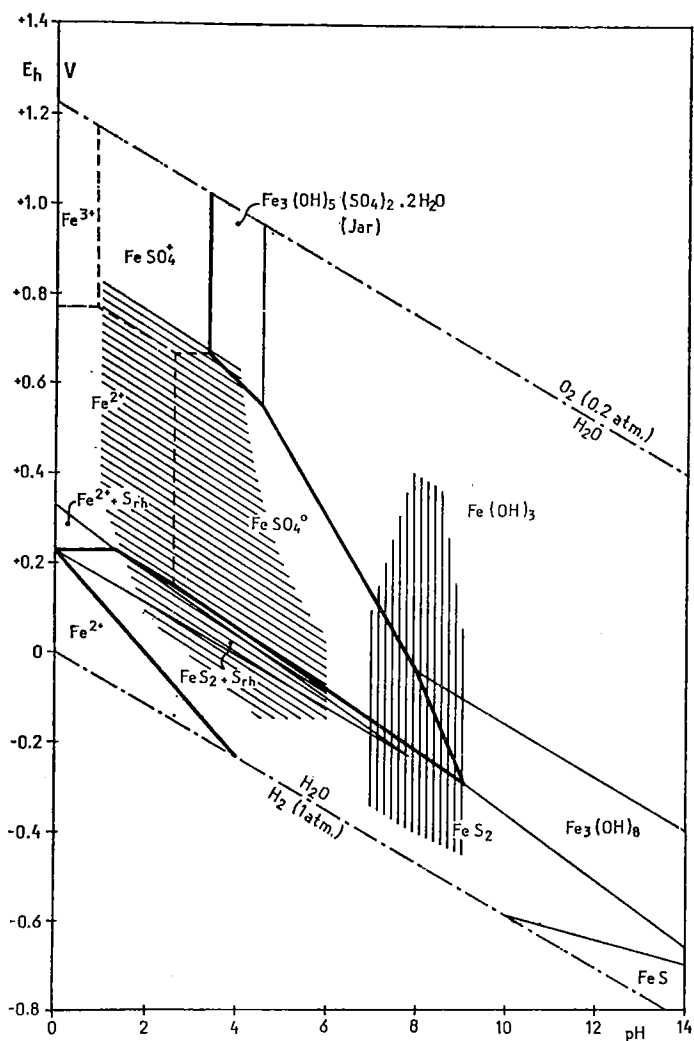


Fig. 2. Eh-pH diagram of iron sulphides and metastable iron hydroxides at 25°C and 1 atm total pressure;  $\Sigma S = 10^{-3}$ . Boundary between solids and ions at an activity of  $10^{-6}$  of dissolved iron species.

Schwertmann, 1961),  $Fe_3O_4$  (magnetite), and  $\alpha$ -FeOOH (goethite). Although  $Fe(OH)_3$  (amorphous ferric hydroxide) and  $Fe_3(OH)_8$  (amorphous ferric-ferrous hydroxide: Ponnampuruma, 1964) are unstable relative to  $\alpha$ -FeOOH and  $Fe_3O_4$ , respectively, they occur as metastable phases in the soils under discussion. The alternating reduction and oxidation, resulting from the fluctuating watertable, continually produce new  $Fe(OH)_3$  (van Breemen & Oldeman, 1967)\*\*, so that

\*\* Breemen, N. van & L. R. Oldeman (1967). Bodemvorming en bodemclassificatie van rijstgronden. Unpublished report.

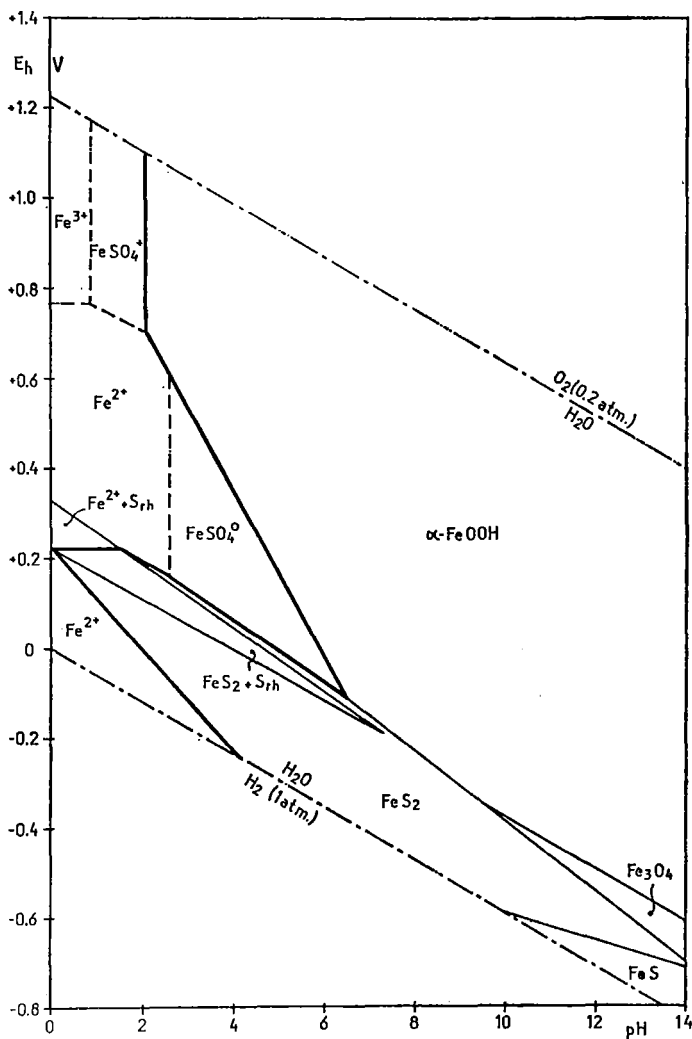


Fig. 3. Eh-pH diagram of iron sulphides and stable iron oxides at 25°C and 1 atm total pressure;  $\Sigma S = 10^{-3}$ . Boundary between solids and ions at an activity of  $10^{-6}$  of dissolved iron compounds.

the reaction  $Fe(OH)_3 \rightarrow \alpha\text{-FeOOH} + H_2O$  is hindered or even reversed.

With this knowledge two Eh-pH diagrams have been constructed, one including metastable iron hydroxides (Fig. 2) and one including the stable iron minerals (Fig. 3). The procedure for the construction of such diagrams can be studied in the book of Garrels & Christ (1965). The equations needed to delineate the stability fields are given in Appendix 3.

Fig. 2 clearly shows that oxidation of  $FeS_2$  may cause formation of jarosite via the dissolved  $FeSO_4^+$ ; possibly rhombic S may be formed as an intermediate phase.

The jarosite is yellow. Leaching of  $H^+$  turns it into brown  $Fe(OH)_3$ . The young soils therefore show yellow mottles, which turn brownish while ageing.

In Fig. 2 two fields are drawn, a vertically hatched one and an obliquely hatched one. The former gives the variations in Eh and pH in marine sediments and the latter those in cat clay soils (van Breemen, 1968). Evidently much of the acid sulphate soils falls in the fields of dissolved iron species. This shows that iron is very mobile in such soils as Tables 1, 7 and 13 have already shown.

Fig. 3 is quite different. The jarosite field has completely disappeared. Equation 31 in Appendix 2 shows that the boundary between goethite and jarosite lies at a pH value of  $-1.05$ , if  $\lg [HSO_4^-] = -3$ . At this pH, however, both phases are metastable, as the ions  $FeSO_4^+$  and  $Fe^{3+}$  are the stable components. If, therefore, oxidation of pyrite leads to formation of crystalline  $\alpha$ - $FeOOH$ , jarosite cannot be formed. The formation of well crystallized goethite is favoured by slow oxidation of ferrous salts at low partial pressures of  $CO_2$  (Schwertmann, 1959), by the absence of dissolved silica (Schellmann, 1959) and by low concentrations of Mg salts in the solution (Schellmann, 1959). These requirements are certainly not fulfilled in acid sulphate soils, and the conditions for the formation of well crystallized goethite in the early stages of pyrite oxidation are therefore not favourable. Consequently, amorphous products are formed and jarosite can be a stable phase. Upon ageing the amorphous hydroxides crystallize into goethite; jarosite disappears.

The soils under consideration have not developed into real cat clays since the original pyrite content was too low and montmorillonites formed part of the clay mineral assemblage. The numerous  $H^+$  ions liberated on oxidation of pyrite are buffered by montmorillonite, partly by its high exchange capacity and partly by its instability in acid medium (see Tables 4, 10 and 16). The  $H^+$  liberates  $Mg^{2+}$  from the lattice, the silicate lattice becomes unstable and the  $H^+$  forms undissociated  $H_4SiO_4^0$  with the silicate; hence the pH of the soils never falls as low as in true cat clays.

In Fig. 3 the field of dissolved iron species is much smaller than in Fig. 2. Thus solid iron species at least partly occur in the amorphous state in acid sulphate soils.

The formation of yellow jarosite in acid sulphate soils is therefore possible only if oxidation of pyrite proceeds rapidly and amorphous iron hydroxides are formed. Upon ageing (leaching) the amorphous brown iron hydroxides crystallize into reddish-brown goethite; jarosite disappears.

## 5 Soil classification

The Kennedy Highway soil (the oldest of the sequence) can be classified according to 1967 edition of the new American soil classification (US Soil Survey Staff, 1960, 1967). The younger two soils, however, do not fall into this system. The latter soils, however, occur in Surinam and also elsewhere over vast areas. This problem was therefore discussed with Dr Guy Smith (January 1968). The result of this discussion is as follows.

The Ma Retraite and Santo soils have a cambic horizon and characteristics associated with wetness. So they should be classified as Inceptisols and more particularly as Aquepts and, since they occur in an isohyperthermic climate, as Tropaquepts. They cannot, however, be placed within the Tropaquepts, since the Tropaquepts should have 'n values of 0.5 or less in some layer between 20 and 50 cm'. This criterion will now be deleted from the definition of the Tropaquepts to place the two soils into this Great Group. Typic Tropaquepts, however, are redefined as to exclude them. Typic Tropaquepts from now on should have 'n values in some layer between 20 and 50 cm which are 0.5 lower'. A new subgroup of Tropaquepts has been called Hydric Tropaquepts and they are defined as follows: 'Tropaquepts like the Typic, with or without any, some or all of the properties of the Fluventic, Histic or Vertic subgroups except for n values'.

## **6 Summary**

The properties and formation of three fine-textured soils with impeded drainage were discussed. The soils occur in the Coastal Plain of Surinam; two lay in the Holocene Young Coastal Plain, the other in the Pleistocene Old Coastal Plain. The three soils form a chronosequence, since all soil forming factors were the same except age.

For each soil, profile descriptions and descriptions of thin sections were presented, together with chemical and X-ray data.

Soil-forming processes were studied by tracing the chemical, physical and mineralogical changes in the soils. The geochemistry of the soils was discussed on the basis of the mineral transformation in relation to the composition of the soil solution and the oxidation-reduction processes of the iron and sulphur compounds.

## **7 Acknowledgments**

The authors are very grateful to Mr W. Saro of the Surinam Soil Survey Department, who participated in the field work, and to Mr A. G. Jongmans and Mr Th. Pape, who assisted in the description of the thin sections. The authors are also indebted to the Director of the Ministry of Mines, Forests and Lands of Surinam for permission to publish this study and to Mr G. E. Kamerling for permission to use some hitherto unpublished data on soil ripening and water permeability.

## Appendix 1

### Profile descriptions and descriptions of thin sections

#### Ma Retraite Profile

Site	Topographical map of Surinam (1963), coordinates N 967.620-E 360.580.
Described by	S. Slager and W. Saro (24.5.1967).
Classification	Hydric Tropaquept (amended from the 1967 Supplement to the 7th Approximation, see Section 5).
Climate	Annual precipitation 2200 mm, two on three months per year with less than 100 mm precipitation; mean annual temperature 27°C with very small daily and monthly variation.
Vegetation	originally <i>Tabebuia</i> sp. and <i>Pterocarpus officinalis</i> ; since 1965 <i>Citrus</i> orchard with <i>Pueraria</i> soil cover.
Parent material	heavy textured Holocene marine clay.
Physiography	alluvial plain, with slightly ponded relief, flat micro-relief and class A slope.
Altitude	about 80 cm above mean sea-level.
Hydrology	a. soil drainage class, before reclamation poorly drained, after reclamation moderately well drained. b. watertable before reclamation: presumed highest 1 m above surface, presumed lowest 1 m below surface; after reclamation rather constant at 80 cm below surface. c. flooding before reclamation every year for 6-8 months with 1 m brackish water; since reclamation no flooding. d. water permeability: between 62 and 103 cm: 11 m between 103 and 128 cm: 10 m between 128 and 140 cm: 17 m between 140 and 152 cm: 3 m per 24 h.

#### *Description of soil horizons and thin sections*

A1g 0-20 cm	very dark-greyish-brown (10YR 3/2) moist clay with common organic matter; strong very fine subangular-
-------------	--

- blocky; common very fine, few moderately fine, common moderately large and few very large biopores; friable; pH (Hellige) 4.5; diffuse and wavy boundary.
- B1g 20-32 cm** dark-greyish-brown (10YR 4/2) moist clay with little organic matter; strong coarse compound rough prismatic subdivided into moderate very fine subangular-blocky; common very fine, few moderately fine, many moderately large, few very large biopores; slightly firm; common, fine faint dark-yellowish-brown (10YR 4/4) (Fe) mottles; pH (Hellige) 4.0; gradual and smooth boundary.
- B21g 32-63 cm** greyish-brown (10YR 5/2) moist clay with very little organic matter; strong very coarse compound rough prismatic subdivided into strong coarse compound rough prismatic subdivided into moderate very fine angular-blocky; common very fine, few to common moderately fine, abundant moderately large and common very large biopores; on 75 % of faces or large prisms, dark-yellowish-brown (10YR 3/4) (Fe) coating; many medium, prominent dark-yellowish-brown (10YR 4/4) (Fe) soft nodules, mainly concentrated along root channels; sticky plastic; pH (Hellige) 4; diffuse and smooth boundary.
- Microstructure:  
 Plasmic fabric: clinobimasepic and channelvosepic.  
 Basic structure: channelvosepic s-matrix with macro-channels up to 0.5 cm diameter; skeleton grains: very few, restricted to silt fraction.  
 Elementary structure: subcutanic channelvosepic. Main pedological feature: channel neosesquans, 50-500  $\mu\text{m}$ , sometimes discontinuous, orange to orange-yellow, related to channel neostrians and channel quasi-jarositans.  
 Primary structure: other pedological features:
1. sesquioxidic glaebules up to 500  $\mu\text{m}$ , very diffuse, strongly adhesive, irregular, orange to yellow-orange.
  2. channel quasi-jarositans few, up to 500  $\mu\text{m}$ , discontinuous; diffuse boundaries; related to channel neostrians and channel neosesquans.
- B22g 63-95 cm** (dark-)grey (10YR 5/1) moist clay; structure as B21g; common very fine, few moderately fine, many to abundant moderately large, common very large biopores; very sticky plastic; on 75 % of faces or large prisms dark-yellowish-brown (10YR 3/4) (Fe) coating; common medium prominent (dark-)brown (7.5YR 4/3) (Fe)

soft nodules concentrated along root channels; few fine distinct pale-yellow (2.5Y 8/4) (S) mottles; pH (Hellige) 4; gradual and smooth boundary.

**B3g +95 cm** dark-grey (5Y 4/1) wet clay; moderate coarse compound smooth prismatic subdivided into weak fine angular-blocky; few very fine, few moderately fine, many moderately large and few to common very large biopores; very sticky and very plastic; soil material shows little resistance when pressed between the hands; common medium distinct very dark-greyish-brown (2.5Y 3/2) (Fe) soft nodules; pH (Hellige) 8.

### **Santo Profile**

**Site** Topographical map of Surinam (1956), coordinates N 959.950-E 345.180.

**Described by** S. Slager and W. Saro (15.8.1967).

**Classification** Hydric Tropaquept (amended from the 1967 Supplement to the 7th Approximation, see Section 5).

**Climate** Mean annual precipitation 2200 mm, two or three months with less than 100 mm; mean annual temperature 27°C with very small daily and monthly variations.

**Land-use** experimental field of bananas.

**Parent material** heavy-textured Holocene marine deposits.

**Physiography** alluvial plain with flat relief, flat microrelief and class A slope.

**Altitude** about 70 cm above present mean sea-level.

**Hydrology** a. soil drainage class: imperfectly drained  
 b. watertable:  
 presumed highest 10 cm below surface  
 presumed lowest 150 cm below surface  
 actual 110 cm below surface

### *Descriptions of soil horizons and thin sections*

**O<sub>1</sub> + O<sub>2</sub> 24-0 cm** dark-reddish-brown (5YR 3/3) moist muck; friable; pH (Hellige) 4; clear and wavy boundary.

**A1g 0-19 cm** very dark-greyish-brown (10YR 3/2) moist clay with much organic matter; strong very fine subangular-blocky and strong very fine granular with common (very) fine biopores; slightly sticky and slightly plastic; pH (Hellige) 4; smooth and gradual boundary.

**Microstructure:**

Plasmic fabric: weak channelvosepic and masepic. Plasma consists of clay and many fine brown and black organic particles.

Basic structure: channelled and vughy vo-masepic matrix with macrochannels and micro and macro vughs; few skeleton grains, restricted to silt fraction.

Elementary structure: glaebular channelled and vughy, weakly vo-masepic; main pedological feature: some organic nodules up to 2 mm, irregular with undifferentiated fabric and sharp to diffuse boundaries.

Primary structure: other pedological features:

a. some organic faecal pellets up to some hundreds of micrometres

b. root remnants.

B1g 19-38 cm

light-grey (N 7/0) moist clay with little organic matter; moderate coarse compound rough prismatic subdivided into strong very fine angular-blocky with many stress cutans; common to few (very) fine biopores within peds, few on ped faces; common moderately large biopores; few very large biopores; slightly sticky and plastic; common fine distinct yellowish-red (5YR 4/6) (Fe) mottles; pH (Hellige) 5.5; gradual and wavy boundary.

Microstructure:

Plasmic fabric: channelvosepic and clinobimasepic.

Basic structure: channelled and fractured vo-masepic. s-matrix with macrochannels and micro and macro skew planes and few skeleton grains, restricted to silt fraction.

Elementary structure: subcutanic channelled and fractured, vo-masepic; main pedological feature: very thin to medium yellow to orange brown channel neosesquans and compound channel neo-quasisesquans with rather sharp to diffuse boundaries.

Primary structure

a. fine to very coarse irregular organic nodules, generally with soil fabric

b. some very diffuse irregular, orange sesquioxidic nodules, up to some millimetres

c. root remnants in most of the channels

d. probably some very thin to thin orange illuviation channel ferriargillans and papules.

B2g 38-65/83 cm

light-grey (N 7/0) moist clay; moderate coarse compound rough prismatic subdivided into strong very fine

angular-blocky with many stress cutans; common (very) fine biopores within peds, very few on ped faces; few large biopores on and within peds; very sticky and plastic; on ped faces, common medium faint yellowish-brown (10YR 5/8) (Fe) mottles; within peds, many medium distinct yellow (10YR 6/8) (Fe) mottles; pH (Hellinge) 5.5; clear and wavy boundary.

Microstructure:

Plasmic fabric: channelvosepic and clinobimasepic.

Basic structure: channelled and planed, channelvosepic. s-matrix with macrochannels and micro and macro skew joint planes; few skeleton grains, restricted to silt fraction, locally clustered.

Elementary structure: subcutanic channelled and planed, channelvosepic; main pedological feature: very thin to medium yellow to orange channel neosesquans with diffuse boundaries.

Primary structure: other pedological features:

- a. fine to extremely coarse yellow to orange irregular sesquioxidic nodules with diffuse boundaries in clusters
- b. some medium to very coarse rather sharply bounded organic nodules
- c. channel quasi-sesquans, orange to brown, diffuse boundaries, 20-50  $\mu\text{m}$  wide
- d. plant remnants at several stages of decay.

B3g 65/83-130(+)  
cm

bluish-grey (5B 5/1) wet clay; strong coarse, compound smooth prismatic subdivided into strong very fine angular-blocky with abundant stress cutans; (very) fine biopores: few within peds, very few on ped faces; large biopores: very few within peds and on ped faces; very sticky and very plastic; on ped faces, few fine faint yellow (10YR 8/8) (Fe) mottles; within peds, common medium distinct light-olive-brown (2.5Y 5/6) (Fe) mottles; pH (Hellige) 7.0.

Microstructure:

Plasmic fabric: channelvosepic, masepic, locally mosepic.

Basic structure: channelled and fractured vomasepic with macrochannels and skew planes; very few skeleton grains, restricted to the silt fraction, sometimes in clusters.

Elementary structure is neocutanic vomasepic s-matrix; main pedological feature: channel neosesquans 20-60  $\mu\text{m}$  wide with undifferentiated fabric, orange-brown to

dark-brown, rather sharp to diffuse boundaries, sometimes related to sesquioxidic nodules.

Primary structure:

a. sesquioxidic glaeboles: ferric nodules with an undifferentiated fabric or a compound fabric, yellowish-brown to dark-brown, discontinuous, irregular to spherical, strongly adhesive, very diffuse to rather sharp boundaries, most of the nodules short distances from channels

b. channel quasisesquans: with undifferentiated fabric, diffuse boundaries, 20-50  $\mu\text{m}$  wide, orange-brown to brown

c. plant remnants in several stages of decay.

### Kennedy Highway Profile

Site	Topographical map of Surinam (1953), coordinates N 934.000-E 354.840.
Described by	S. Slager and W. Saro (28.9.1967).
Classification	Plinthaquult (7th Approximation, 1967).
Climate	mean annual precipitation 2200 mm with two or three months per year with less than 100 mm; mean annual temperature 27°C with very small daily and monthly variation.
Land-use	shifting cultivation.
Parent material	medium to heavy textured Pleistocene marine deposits.
Physiography	slightly elevated plateau with flat relief and flat micro-relief and class A slope.
Altitude	about 7 m above present mean sea-level.
Hydrology	a. soil drainage class: imperfectly drained b. watertable: presumed highest near surface; presumed lowest about 200 cm below the soil surface; actual watertable 130 cm below surface.

### *Description of soil horizons and thin sections*

A11 0-24 cm	dark-greyish-brown (10YR 4/2) moist silt-loam with little organic matter and little fine faint charcoal; strong very fine subangular-blocky with few (very) fine biopores; friable; pH (Hellige) 4; gradual and smooth boundary.
A12g 24-41 cm	grey (10YR 6/1) moist silty clay-loam with common organic matter; strong very fine subangular-blocky with

few (very) fine biopores; slightly firm; pH (Hellige) 4; clear and wavy boundary.

B1tg 41-77 cm

grey (10YR 6/1) moist silty clay; strong very fine, angular-blocky with many stress cutans; very few (very) fine biopores; sticky slightly plastic; common large distinct red (10R 4/8) and common medium distinct yellowish-red (5R 5/8) iron mottles; pH (Hellige) 4; gradual and smooth boundary.

B21tg 77-104 cm

(light-)gray (5Y 6.5/1) moist clay; strong fine angular-blocky with many stress cutans; very few (very) fine biopores; sticky, slightly plastic; common medium prominent red (10R 4/8) and many medium distinct reddish-yellow (7.5YR 7/8) soft iron mottles; pH (Hellige) 4; smooth and clear boundary.

Microstructure:

Plasmic fabric: vo, ma, and mo sepic.

Basic structure: porphyroskelic s matrix with craze, skew and joint planes and macrochannels. Skeleton grains very few, mainly quartz and some resistant minerals, from 2 to 100  $\mu\text{m}$ , fairly rounded.

Elementary structure: glaebular crazed porphyroskelic; main pedological feature: sesquioxidic nodules, some micrometres to millimetres, orange to red, boundaries from very sharp to very diffuse, spherical to compound cracked with irregular boundary; if compound, with strong variation in iron content; nodules are associated with either channels and planes or to sesquans, neosesquans and quasisesquans; the red nodules consist of many extremely fine red birefringent droplets which concentrate near the centre of the nodule.

Primary structure: other pedological features:

a. papules: some tens to hundreds of micrometres in size, whitish-yellow birefringent, moderate to strong orientation, covering some 4 % of the area of the thin section

b. sesquans: discontinuous reddish-brown and dark-red plane sesquans, some tens of micrometres thick, generally related to sesquioxidic nodules, occurring as sesquioxidic crystal sheets if the planes are closed

c. neosesquans: plane and channel neosesquans, some tens to hundreds of micrometres, yellow, brown to dark-red birefringent, related to and merging into sesquioxidic nodules

B22tg 104-135 cm

d. quasisesquans: channel quasisesquans, yellow to red birefringent, related to sesquioxidic nodules. (light-)grey (5Y 6/1) wet silty clay; strong fine, angular-blocky with many stress cutans; very few (very) fine biopores; sticky and plastic; abundant large prominent dark-red (7.5R 3/8) soft and hard nodules; common medium faint reddish-yellow (5YR 6/8) iron mottles; pH (Hellige) 4.

## Appendix 2

Using the symbols Or for potassium feldspar ( $\text{KAlSi}_3\text{O}_8$ ), Ms for muscovite ( $\text{KA}_3\text{Si}_3\text{O}_{10}(\text{OH})_2$ ), Pyr for pyrophyllite ( $\text{Al}_2\text{Si}_4\text{O}_{10}(\text{OH})_2$ ), Kaol for kaolinite ( $\text{Al}_2\text{Si}_2\text{O}_5(\text{OH})_2$ ) and Gibb for gibbsite ( $\text{Al}_2\text{O}_3 \cdot 3\text{H}_2\text{O}$ ) the reactions needed to establish the stability of the phases in the system  $\text{K}_2\text{O}-\text{Al}_2\text{O}_3-\text{SiO}_2-\text{H}_2\text{O}$  are, with the charges of the ions omitted:



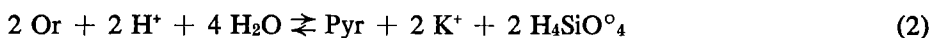
$$K_1 = \frac{[\text{Ms}] [\text{K}]^2 [\text{H}_4\text{SiO}_4]^6}{[\text{Or}]^3 [\text{H}]^2 [\text{H}_2\text{O}]^{12}},$$

where square brackets denote activities. As, by convention, the activities of solid substances are taken to be unity, and as, in dilute solutions, the activity of water is also unity, the expression for  $K_1$  reduces to:

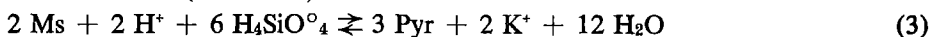
$$K_1 = \frac{[\text{K}]^2 [\text{H}_4\text{SiO}_4]^6}{[\text{H}]^2}, \text{ or}$$

$$\lg K_1 = 2 \lg \left\{ \frac{[\text{K}]}{[\text{H}]} \right\} + 6 \lg [\text{H}_4\text{SiO}_4] \quad (1a)$$

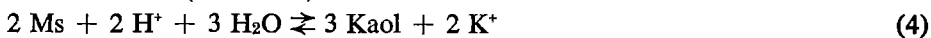
Similarly:



$$\lg K_2 = 2 \lg \left\{ \frac{[\text{K}]}{[\text{H}]} \right\} + 2 \lg [\text{H}_4\text{SiO}_4] \quad (2a)$$



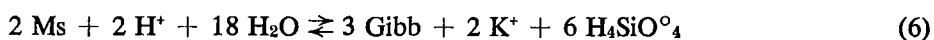
$$\lg K_3 = 2 \lg \left\{ \frac{[\text{K}]}{[\text{H}]} \right\} - 6 \lg [\text{H}_4\text{SiO}_4] \quad (3a)$$



$$\lg K_4 = 2 \lg \left\{ \frac{[\text{K}]}{[\text{H}]} \right\} \quad (4a)$$



$$\lg K_5 = 2 \lg [\text{H}_4\text{SiO}_4] \quad (5a)$$



$$\lg K_6 = 2 \lg \left\{ \frac{[\text{K}]}{[\text{H}]} \right\} + 6 \lg [\text{H}_4\text{SiO}_4] \quad (6a)$$



$$\lg K_7 = 2 \lg [\text{H}_4\text{SiO}_4] \quad (7a)$$

To calculate the thermodynamic equilibrium constants, the following relations have to be used:

$$\ln K = -\Delta F_r^\circ/RT \quad \text{or} \quad \lg K = -\Delta F_r^\circ/1.364 \quad (8)$$

and

$$\Delta F_r^\circ = (\sum \Delta F_f^\circ)_{\text{products}} - (\sum \Delta F_f^\circ)_{\text{reactants}} \quad (9)$$

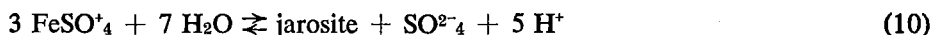
where K is the equilibrium constant,  $\Delta F_r^\circ$  the standard free energy change of the reaction,  $\Delta F_f^\circ$  the standard free energy of formation, R the gas constant (0.001987 kcal/°K) and T the absolute temperature (298.15°K = 25°C). All reactions are considered to proceed at 1 atm.

The values used for the standard free energy of formation are  $\Delta F_f^\circ \text{Or} = -893.8$  (Kelley, 1962),  $\Delta F_f^\circ \text{Ms} = -1330.1$  (Barany, 1964),  $\Delta F_f^\circ \text{Pyr} = -1258.7$  (Reesman & Keller, 1968),  $\Delta F_f^\circ \text{Kaol} = -904.0$  (ibid.),  $\Delta F_f^\circ \text{Gibb} = -547.0$  (Barany & Kelly, 1961),  $\Delta F_f^\circ \text{H}_4\text{SiO}_4 = -312.7$  (Reesman & Keller, l.c.),  $\Delta F_f^\circ \text{K}^+ = -67.5$  (Rossini *et al.*, 1952),  $\Delta F_f^\circ \text{H}_2\text{O} = -56.7$  (ibid.) and  $\Delta F_f^\circ \text{H}^+ = 0$ , all values in kcal/mol. With (9) and (8) the following values for lg K were obtained: lg K<sub>1</sub> = -15.4, lg K<sub>2</sub> = +3.3, lg K<sub>3</sub> = +40.5, lg K<sub>4</sub> = +12.2, lg K<sub>5</sub> = -9.4, lg K<sub>6</sub> = -21.2, lg K<sub>7</sub> = -11.2.

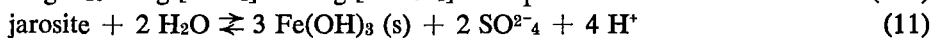
With these data, the stability fields of the minerals could be represented in a two-dimensional diagram with  $\lg \left\{ \frac{[\text{K}]}{[\text{H}]} \right\}$  on one axis and  $\lg [\text{H}_4\text{SiO}_4]$  on the other (Fig. 1). The line of highest quantity of dissolved silica,  $10^{-2.8} \text{mol l}^{-1}$ , was obtained from Siever's data (1962). At the right of this line is therefore the field of potassium feldspar + amorphous silica.

### Appendix 3

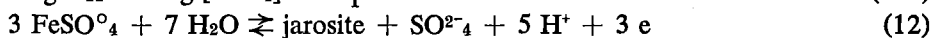
The stability fields of the phases occurring in the Eh-pH diagram represented in Fig. 2, are based on the following redox and other reactions:



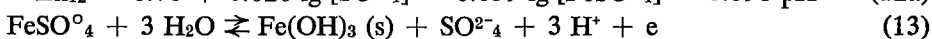
$$\lg K_{10} = \lg [\text{SO}_4^{2-}] - 3 \lg [\text{FeSO}_4^+] - 5 \text{pH} = -1.9 \quad (10a)$$



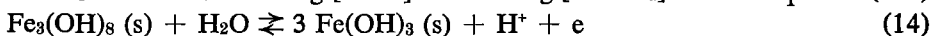
$$\lg K_{11} = 2 \lg [\text{SO}_4^{2-}] - 4 \text{pH} = -24.6 \quad (11a)$$



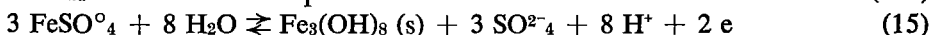
$$\text{Eh}_{12} = 0.70 + 0.020 \lg [\text{SO}_4^{2-}] - 0.059 \lg [\text{FeSO}_4^{\circ}] - 0.098 \text{pH} \quad (12a)$$



$$\text{Eh}_{13} = 1.17 + 0.059 \lg [\text{SO}_4^{2-}] - 0.059 \lg [\text{FeSO}_4^{\circ}] - 0.177 \text{pH} \quad (13a)$$



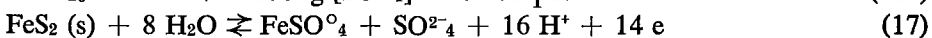
$$\text{Eh}_{14} = 0.43 - 0.059 \text{pH} \quad (14a)$$



$$\text{Eh}_{15} = 1.58 + 0.089 \lg [\text{SO}_4^{2-}] - 0.089 \lg [\text{FeSO}_4^{\circ}] - 0.236 \text{pH} \quad (15a)$$



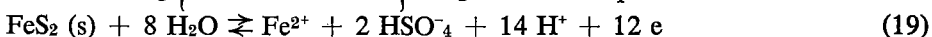
$$\text{Eh}_{16} = 0.41 + 0.008 \lg [\text{SO}_4^{2-}] - 0.075 \text{pH} \quad (16a)$$



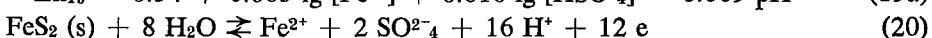
$$\text{Eh}_{17} = 0.36 + 0.004 \lg [\text{FeSO}_4^{\circ}] + 0.004 \lg [\text{SO}_4^{2-}] - 0.067 \text{pH} \quad (17a)$$



$$\lg K_{18} = \lg \left\{ \frac{[\text{FeSO}_4^{\circ}]}{[\text{Fe}^{2+}]} \right\} - \lg [\text{HSO}_4^-] - \text{pH} = 0.4 \quad (18a)$$



$$\text{Eh}_{19} = 0.34 + 0.005 \lg [\text{Fe}^{2+}] + 0.010 \lg [\text{HSO}_4^-] - 0.069 \text{pH} \quad (19a)$$



$$\text{Eh}_{20} = 0.41 + 0.005 \lg [\text{Fe}^{2+}] + 0.010 \lg [\text{SO}_4^{2-}] - 0.079 \text{pH} \quad (20a)$$



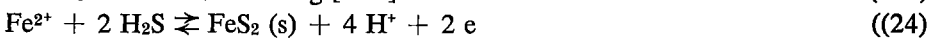
$$\text{Eh}_{21} = 0.14 - 0.030 \lg [\text{H}_2\text{S}] - 0.059 \text{pH} \quad (21a)$$



$$\text{Eh}_{22} = 0.34 + 0.010 \lg [\text{HSO}_4^-] - 0.069 \text{pH} \quad (22a)$$



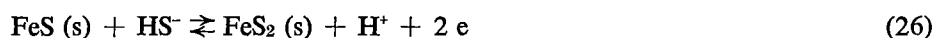
$$\text{Eh}_{23} = 0.40 + 0.030 \lg [\text{Fe}^{2+}] \quad (23a)$$



$$\text{Eh}_{24} = -0.12 - 0.059 \lg [\text{H}_2\text{S}] - 0.030 \lg [\text{Fe}^{2+}] - 0.118 \text{pH} \quad (24a)$$



$$\text{Eh}_{25} = 0.36 + 0.010 \lg [\text{SO}_4^{2-}] - 0.079 \text{pH} \quad (25a)$$



$$\text{Eh}_{26} = -0.38 - 0.030 \lg [\text{HS}^-] - 0.030 \text{ pH} \quad (26a)$$



$$\lg K_{27} = \lg \left\{ \frac{[\text{FeSO}_4^+]}{[\text{Fe}^{3+}]} \right\} - \lg [\text{HSO}_4^-] - \text{pH} = 2.1 \quad (27a)$$



$$\text{Eh}_{28} = 0.67 + 0.059 \lg \left\{ \frac{[\text{FeSO}_4^+]}{[\text{FeSO}_4^{\circ}]} \right\} \quad (28a)$$



$$\text{Eh}_{29} = 0.64 - 0.059 \lg \left\{ \frac{[\text{FeSO}_4^+]}{[\text{Fe}^{2+}]} \right\} - 0.059 \lg [\text{HSO}_4^-] - 0.059 \text{ pH} \quad (29a)$$

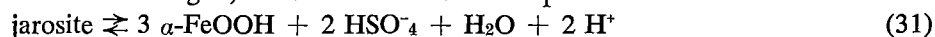


$$\text{Eh}_{30} = 0.77 + 0.059 \lg \left\{ \frac{[\text{Fe}^{3+}]}{[\text{Fe}^{2+}]} \right\} \quad (30a)$$

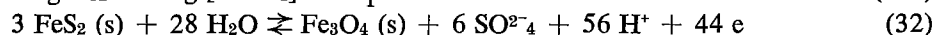
In these equations brackets denote activities;  $S_{\text{rh}}$  means rhombic sulphur.

The values for  $\lg K$  were obtained in the way described in Appendix 2; those for the standard redox potentials from  $\text{Eh}^{\circ} = \Delta F^{\circ}_f/nF$  with  $F = 23.06$  kcal per Volt-gram equivalent and  $n$  the number of electrons formed in oxidation. Most values of  $\Delta F^{\circ}_f$  were taken from Garrels & Christ (1965), those of  $\text{FeSO}_4^{\circ}$  ( $-200.8$  kcal/mol),  $\text{FeSO}_4^+$  ( $-185.4$  kcal/mol) and jarosite ( $-773.0$  kcal/mol) from van Breemen (1968)\*, the  $\Delta F^{\circ}_f$  value of  $\text{Fe}_3(\text{OH})_8$  ( $-451.2$  kcal/mol) from Ponnampuruma *et al.* (1967).

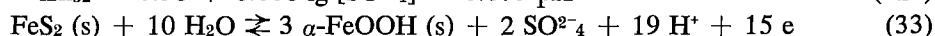
To construct Fig. 3, some additional redox couples were needed:



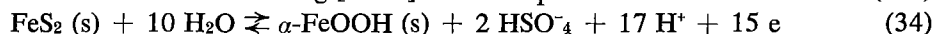
$$\lg K_{31} = 2 \lg [\text{HSO}_4^-] - 2 \text{ pH} = -3.9 \quad (31a)$$



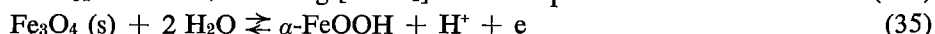
$$\text{Eh}_{32} = 0.38 + 0.008 \lg [\text{SO}_4^{2-}] - 0.075 \text{ pH} \quad (32a)$$



$$\text{Eh}_{33} = 0.38 + 0.008 \lg [\text{SO}_4^{2-}] - 0.075 \text{ pH} \quad (33a)$$



$$\text{Eh}_{34} = 0.37 + 0.008 \lg [\text{HSO}_4^-] - 0.067 \text{ pH} \quad (34a)$$



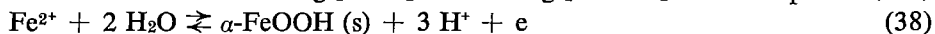
$$\text{Eh}_{35} = 0.21 - 0.059 \text{ pH} \quad (35a)$$



$$\lg K_{36} = \lg [\text{SO}_4^{2-}] - \lg [\text{FeSO}_4^+] - 3 \text{ pH} = -3.3 \quad (36a)$$



$$\text{Eh}_{37} = 0.86 + 0.059 \lg [\text{SO}_4^{2-}] - 0.059 \lg [\text{FeSO}_4^{\circ}] - 0.177 \text{ pH} \quad (37a)$$



$$\text{Eh}_{38} = 0.73 - 0.059 \lg [\text{Fe}^{2+}] - 0.177 \text{ pH} \quad (38a)$$

The standard free energy of formation of goethite was taken from Schmalz (1959).

\* See note on page 15

## References

- Amson, F. A. van 1966 Some aspects of clay soils in the Demerara formation of Surinam. Bull. LandbProefstn Suriname 84.
- Barany, R. 1964 Heat and free-energy of formation of muscovite. Rep. Invest. U.S. Bur. Mines 6356.
- Barany, R. & 1961 Heats and free-energies of formation of gibbsite, kaolinite, halloysite, and dickite. Rep. Invest. U.S. Bur. Mines 5825.  
K. K. Kelley
- Barshad, I. 1960 Significance of the presence of exchangeable magnesium in acidified clays. Science, N.Y. 131: 988-90.
- Berner, R. A. 1964 Iron sulfides formed from aqueous solutions at low temperatures and atmospheric pressure. J. Geol. 72: 293-306.
- Bouma, J., L. J. Pons & 1968 On soil genesis in temperate humid climate. VI. The formation of a glossudalf in loess (silt loam). Neth. J. agric. Sci. 16: 58-70.  
J. van Schuylenborgh
- Brinkman, R. & 1968 A pedo-geomorphological classification and map of the holocene sediments in the coastal plain of the three Guianas. Soil Surv. Pap., Neth. Soil Surv. Inst. 4.  
L. J. Pons
- Brewer, R. 1964 Fabric and mineral analysis of soils. New York.
- Diephuis, J. G. H. R. 1966 The Guiana coast. Tijdschr. K. ned. aardrijksk. Genoot. 83: 145-53.
- Es, F. W. J. van & 1967 Contribution to the knowledge of a solonetzic, magnesium-rich, alluvial silty clay in the Maro-Koembe plain. Neth. J. agric. Sci. 15: 11-20.  
J. van Schuylenborgh
- Evans, H. T., Ch. Milton, 1964 Valleriite and the new iron sulfide, mackinawite. Prof. Pap. U.S. geol. Surv. 475D: 64-9.  
E. C. T. Chao, I. Adler,  
C. Mead, B. Ingram &  
R. A. Berner
- Eyk, J. J. van der 1957 Reconnaissance soil survey in northern Surinam. Thesis Wageningen.
- Garrels, R. M. & 1965 Solutions, minerals, and equilibria. London.  
Ch. L. Christ
- Hallsworth, E. G. 1963 An examination of some factors affecting the movement of clay in an artificial soil. J. Soil Sci. 14: 360-71.
- Jongerijs, A. 1957 Morfologische studies over de bodemstructuur. Thesis Wageningen. VLO 63.12.
- Jongerijs, A. & 1964 The preparation of mammoth sized thin sections. Soil Surv. Pap., Neth. Soil Surv. Inst. 1.  
G. Heintzberger
- Kelley, K. K. 1962 Heats and free-energies of formation of anhydrous silicates. Rep. Invest. U.S. Bur. Mines 5901.
- Levelt, Th. W. M. & 1968 Some results of profile drilling along the railroad between Onverwacht and Zanderij, Surinam. Geologie Mijnb. 47: 340-5.  
J. Quakernaat

490

Montagne, D. G. 1964 New facts on the geology of the young, unconsolidated sediments of northern Surinam. *Geologie Mijnb.* 43: 499-515.

Nhung, N. N. & F. N. Ponnampereuma 1966 Effects of calcium carbonate, manganese dioxide, ferric hydroxide and prolonged flooding on chemical and electrochemical changes and growth of rice in a flooded acid sulfate soil. *Soil Sci.* 102: 29-41.

Plas, L. van der & J. van Schuylenborgh 1970 Petrochemical calculations applied to soils. *Geoderma* (in preparation).

Ponnampereuma, F. N., E. M. Tianco & T. Loy 1967 Redox equilibria in flooded soils. I. The iron hydroxide system. *Soil Sci.* 103: 374-82.

Pons, L. J. 1964 A quantitative microscopical method of pyrite determination in soils. In: A. Jongerius (ed.) *Soil Micromorphology*. Elsevier Publ. Co., Amsterdam, 401-409.

Pons, L. J. 1966 Geogenese en pedogenese in de Jong-Holocene kustvlakte van de drie Guianas. *Tijdschr. K. ned. aandr. Genoot* 83: 153-73.

Pons, L. J. & I. S. Zonneveld 1965 Soil ripening and soil classification. *Publs int. Inst. Ld Reclam. Improv.* 13.

Reesman, A. L. & W. D. Keller 1968 Aqueous solubility studies of high-alumina and clay minerals. *Am. Miner.* 53: 929-42.

Rossini, F. D., D. D. Wagman, W. A. Evans, S. Levine & I. Jaffe 1952 Selected values of chemical thermodynamic properties. *Circ. U.S. natn. Bur. Stand.* 500.

Schellmann, W. 1959 Experimentelle Untersuchungen über die sedimentäre Bildung von Goethit und Hämatit. *Chemie Erde* 20: 104-35.

Schmalz, R. F. 1959 A note on the system  $Fe_2O_3-H_2O$ . *J. geophys. Res.* 64: 575-9.

Schwertmann, U. 1959 Über die Synthese definierter Eisenoxyde unter verschiedenen Bedingungen. *Z. anorg. allg. Chem.* 298: 337-48.

Schwertmann, U. 1961 Über das Vorkommen und die Entstehung von Jarosit in Marschböden (Maibolt). *Die Naturwissenschaft* 6: 159-160.

Siever, R. 1962 Silica solubility, 0-200°C, and the diagenesis of siliceous sediments. *J. Geol.* 70: 127-50.

Slager, S. 1966 Morphological studies of some cultivated soils. Thesis Wageningen. VLO 670.

Slager, S. & J. P. Schulz 1969 A study on the suitability of some soils in northern Surinam for *Pinus caribaea*, var. *hondurensis*. *Neth. J. agric. Sci.* 17: 92-98.

Spek, J. van der 1950 Katteklei. *Versl. Landbouwk. Onderz.* 56.2.

U.S. Department of Agriculture 1962 Handbook 18: Soil Survey Manual.

U.S. Soil Survey Staff Soil classification. 7th Approximation (1960) and Supplement (1967).

Yoneda, S. & N. Kawada 1954 A study on polder soils in Japan. 5. A note on the forming process of the strong acid soils found in halogenetic polders. *J. Sci. Soil Manure* 25: 36-40.

ISBN 90 220 0194 6